PERTURBATION OF THE PHASES OF TAYLOR FIELD SAMPLES IN THE SYNTHESIS OF LINEAR AND CIRCULAR ARRAY ANTENNAS

J. C. Brégains(1) (Student Member IEEE), F. Ares(1) (Senior Member, IEEE), and A. G. Roederer(2) (Fellow, IEEE).

(1) Radiating Systems Group, Department of Applied Physics,
15782 Campus Sur, Univ. of Santiago de Compostela (Spain)
E-mails: (Ares) faares@usc.es - (Brégains) fajulio@usc.es
(2) European Space Agency, Electromagnetics Division
P.O. Box 299 NL-2200 AG Noordwijk (The Netherlands) – E-mail: Antoine.Roederer@esa.int

ABSTRACT

Antenna design specifications do not usually restrict the phase of the radiated field. Antenna synthesis techniques generally exploit this freedom only indirectly, but direct phase perturbation can be fruitful.

1. INTRODUCTION

Antennas are required to radiate power patterns with given characteristics, but in most cases no restrictions are placed upon the phase of the radiated field. This freedom can be exploited in antenna synthesis either directly, by varying field phases at sample points and calculating the aperture distribution from these perturbed field samples [1,2], or indirectly by simply allowing the field phase to vary as the result of direct variation of other control parameters. Previous direct methods have varied Woodward-Lawson patterns [1,2], but they are limited to planar arrays with rectangular lattices. Here we describe methods that combine the direct and indirect approaches in varying continuous Taylor distributions that are sampled onto linear arrays or circular arrays consisting of concentric rings of elements. These methods are illustrated by application to the synthesis of arrays of elements that, to reduce mutual coupling, are separated by at least 0.7λ.

2. THEORY

2.1. LINEAR ARRAYS

Linear array antennas with relatively smooth excitation distributions generating patterns with desired characteristics can be synthesized by a method based on perturbation of the zeros u_n of a Taylor pattern $F(u)$, where $u = (2a/\lambda)\cos\theta$ ($2a$ being the length of the corresponding Taylor line source and θ the angle from endfire) [3]. In the present approach we also, simultaneously, vary the phases of the field samples that are used to reconstruct the aperture distribution, i.e. the phase shifts δ_m in

$$g(\zeta) = \frac{1}{2a}\left[F(0)e^{j\delta_0} + 2\sum_{m=1}^{\bar{n}-1} F(m)e^{j\delta_m}\cos(m\zeta)\right] \quad (1)$$

where ζ is distance to the right of the centre of the aperture and $\bar{n}$ -1 is the number of controlled side lobes. In each iteration of the search process (performed, as in [3], using simulated annealing to minimize a cost function reflecting the relevant characteristics of the pattern and of the array distribution), the continuous distribution $g(\zeta)$ is sampled onto a linear array of N equispaced radiating elements located between $\zeta = -a$ and $\zeta = a$, the corresponding radiated power pattern is calculated, and the cost function is computed.

2.2. CONCENTRIC RINGS OF ELEMENTS

In this case we perturb the zeros u_n of a continuous circular Taylor pattern $F(u)$ [3] and, in addition, the phase shifts δ_m in the corresponding expression for the aperture distribution,

$$g(p) = \frac{2}{\pi^2}\sum_{m=0}^{\bar{n}-1} \frac{F(\gamma_{1m})e^{j\delta_m} J_0(\gamma_{1m}p)}{[J_0(\gamma_{1m}\pi)]^2} \quad (2)$$

where J_0 is the zeroth-order Bessel function of the first kind, $\pi\gamma_{1m}$ is the m-th root of the first-order Bessel function of the first kind, and $p = \pi\rho/a$, ρ being distance from the centre of the aperture of radius a. In each iteration of the optimization process, the distribution constructed using eq.(2) is sampled onto an array consisting of concentric rings of equispaced elements lying in the xy plane, the excitation of the elements of the innermost ring taking the value $g(0)$ and those of the outermost ring $g(\pi)$.

3. EXAMPLES

3.1. A LINEAR ARRAY

We considered the synthesis of a linear array with 19 elements a distance 0.7λ apart that is required to generate a 20 dB Chebyshev-like pattern and to have an aperture distribution that lacks marked edge-brightening and is generally as smooth as possible in both amplitude and phase. These requirements were imposed by using the cost function

$$C = c_1(SLL_{\max} - SLL_{\max,d})^2 + c_2(SLL_{\min} - SLL_{\min,d})^2 + c_3\left(|I_n|/|I_{n\pm1}|\right)_{max} + c_4\left[\arg(I_n) - \arg(I_{n\pm1})\right]_{max} \qquad (3)$$

where $SLL_{\min}$ and $SLL_{\max}$ are the levels of the lowest and highest side lobes (in dB relative to the main beam), $SLL_{\min,d}$ = $SLL_{\max,d}$ = -20, I_n is the excitation of the n-th radiating element, and the c_i are control weights. Proceeding as described in Section 2.1 above with $\bar{n}$ = 15 led to the pattern and aperture distribution that are compared with those of the conventional Chebyshev distribution in Fig.1 and Table 1. Varying only the zeros u_n of $F(u)$, i.e. fixing $\delta_m = 0$ in eq.(1), led to significantly poorer results, especially as regards the smoothness of the aperture distribution (see Table 1).

3.2. CONCENTRIC RINGS OF ELEMENTS

We considered an array consisting of ten concentric rings numbered k = 1 to 10 from innermost to outermost, each comprising $4k$ equispaced radiating elements with an element factor of $\cos^{0.753}\theta$ giving an element directivity of 7 dB. The distance between neighbouring rings (i.e. between the circles on which the centres of their elements lay) was 0.7λ. In this case we aimed to achieve a smooth distribution generating a 25 dB pencil beam by using the cost function

$$C = c_1 \Delta_{SLL}^2 \, H(\Delta_{SLL}) + c_2 \left(|I_n| / |I_{n\pm1}| \right)_{max} \quad (4)$$

where ΔSLL = (SLL_{max} + 25) and H is the Heaviside step function. Fig.2 compares the ϕ = 0° planes of the most efficient discretized -25 dB Taylor pattern ($\bar{n}$ = 5; dotted curve) and the result of proceeding as described in Section 2.2 above, likewise with $\bar{n}$ = 5 (dashed curve); fixing δ_m = 0 gave results very similar to the Taylor solution (Table 2). All these patterns display large grating lobes due to the large distances between radiating elements. To palliate this, we adapted a symmetry-destroying procedure due to Agrawal [4], rotating the rings of the antenna individually by angles α_k that were optimized simultaneously with the u_n and δ_m. This led to the pattern plotted in Fig.2 as a continuous curve; the corresponding excitation amplitudes and phases are compared in Fig.3 with those of the 25 dB Taylor distribution for $\bar{n}$ = 5; the optimized ring rotation angles α_k were 5.09º, -1.36º, 0.19º, -1.60º, 18.74º, 6.88º, 8.04º, 3.65º, 9.97º and -3.79º for k = 1 to 10, respectively (minus indicates clockwise angle). The initial excitation configuration of this particular example was selected taking into account that $\bar{n}$ = 5 and SLL = -25 dB corresponds to the circular Taylor distribution with optimum efficiency [5]. Nevertheless, if any other configuration that provides initial severe edge-brightening is considered, a marked improvement of the amplitude distribution is perceived after the proposed method is applied.

4. CONCLUSION

Direct perturbation of field sample phases in addition to other control parameters can significantly improve the results achieved by optimization methods in the synthesis of array antennas. As can be seen, edge-brightening is significantly less severe with the new method than in the Chebyshev distribution for linear arrays. This gain has a price: a slight loss of directivity and the need for the element excitations to have different phases (though only within quite a narrow range). With regard to planar arrays, the new method reduces edge-brightening, lowers grating lobes to below the admissible side lobe level, and marginally increases directivity, all at the expense of having to use element excitations with phases that differ from each other (in the considered example only within a range of about 1 degree).

REFERENCES

[1] J. M. Cid, J. A. Rodríguez, and F. Ares: "Shaped Power Patterns Produced by Equispaced Linear Arrays: Optimized Synthesis Using Orthogonal sin(Nx)/sin(x) Beams", *Journal of Electromagnetic Waves and Applications*, Vol. 13, pp. 985-992, 1999.

[2] J. M. Cid, J. A. Rodríguez, F. Ares, and E. Moreno: "Synthesis of Satellite Footprints by Perturbation of Woodward-Lawson Solutions for Planar Array Antennas", *Journal of Electromagnetic Waves and Applications*, Vol. 14, pp. 3-10, 2000.

[3] J. A. Rodríguez, and F. Ares: "Smooth, Efficient Real Amplitude Distributions with no Edge-brightening for Linear and Circular Near-Taylor Sum Patterns", *Electronics Letters*, Vol. 34, pp. 611-612, April 1998.

[4] V. D. Agrawal: "Grating-Lobe Suppression in Phased Arrays by Subarray Rotation", *Proceedings of the IEEE*, Vol. 66, pp. 347-349, March 1978.

[5] R. S. Elliott "Antenna Theory and Design", Wiley Interscience, revised edition, 2003.

LEGENDS FOR FIGURES AND TABLES

LEGENDS FOR THE TABLES

Table 1. Performance of the linear arrays (*: % with respect to the Chebyshev solution).

Table 2. Performance of the circular arrays, with % improvement relative to the Taylor solution in parentheses.

LEGENDS FOR THE FIGURES

Figure 1. Excitation distributions of linear arrays of nineteen 0.7λ-spaced elements generating Chebyshev or Chebyshev-like patterns. Circles indicate amplitudes, triangles phases; hollow symbols indicate the Chebyshev solution, solid symbols the solution optimized as in Section 2.1 with $\bar{n}$ = 15.

Figure 2. Sections in the ϕ = 0º plane of the power patterns of arrays of 220 elements arranged in 10 concentric rings 0.7λ apart. …… 25 dB Taylor, $\bar{n}$ = 5; ---- optimized varying u_n, as described in Section 2.2, with $\bar{n}$ = 5; — as for ----, but optimizing ring rotation angles α_k, as well as δ_m.

Figure 3. The excitation distributions generating the Taylor and fully optimized patterns of Fig.2. Circles indicate amplitudes, triangles phases; hollow symbols indicate the 25 dB Taylor solution with $\bar{n}$ = 5, solid symbols the fully optimized solution.

TABLES

Table 1

	Chebyshev	Varying u_n and δ_n (Improvement)*	Varying u_n only (Improvement)*
Directivity	24.53	23.41 (-4.6)	23.89 (-2.6)
$\|I_{max}\|/\|I_{min}\|$	2.08	1.77 (14.9)	2.39 (-14.9)
$(\|I_n\|/\|I_{n\pm1}\|)_{max}$	2.05	1.22 (40.5)	2.00 (2.4)
Half Power Beamwidth (º)	3.98	3.98 (0.0)	3.98 (0.0)
Beamwidth at 1st null (º)	9.70	10.00 (-3.1)	10.2 (-5.2)
SLL_{max}-SLL_{min} **(dB)**	0.00	0.70 (3.09)	1.5 (5.15)

Table 2

	Taylor -25 dB, $\bar{n}$ = 5	Parameters Varied		
		u_n, δ_m and α_k	u_n and δ_m	u_n
Directivity	1276	1282 (0.5)	1263 (-1.0)	1263 (-1.0)
$\|I_{max}\|/\|I_{min}\|$	2.24	2.12 (5.35)	2.32 (-3.57)	2.33 (-4 %)
$(\|I_n\|/\|I_{n\pm1}\|)_{max}$	1.30	1.14 (12.3)	1.14 (12.3)	1.14 (12.3)
Half Power Beamwidth (º)	4.30	4.36	4.36	4.40
Beamwidth at 1st null (º)	10.80	10.80	11.16	11.22
Grating lobe level (dB)	-14.74	-24.20	-14.64	-14.80

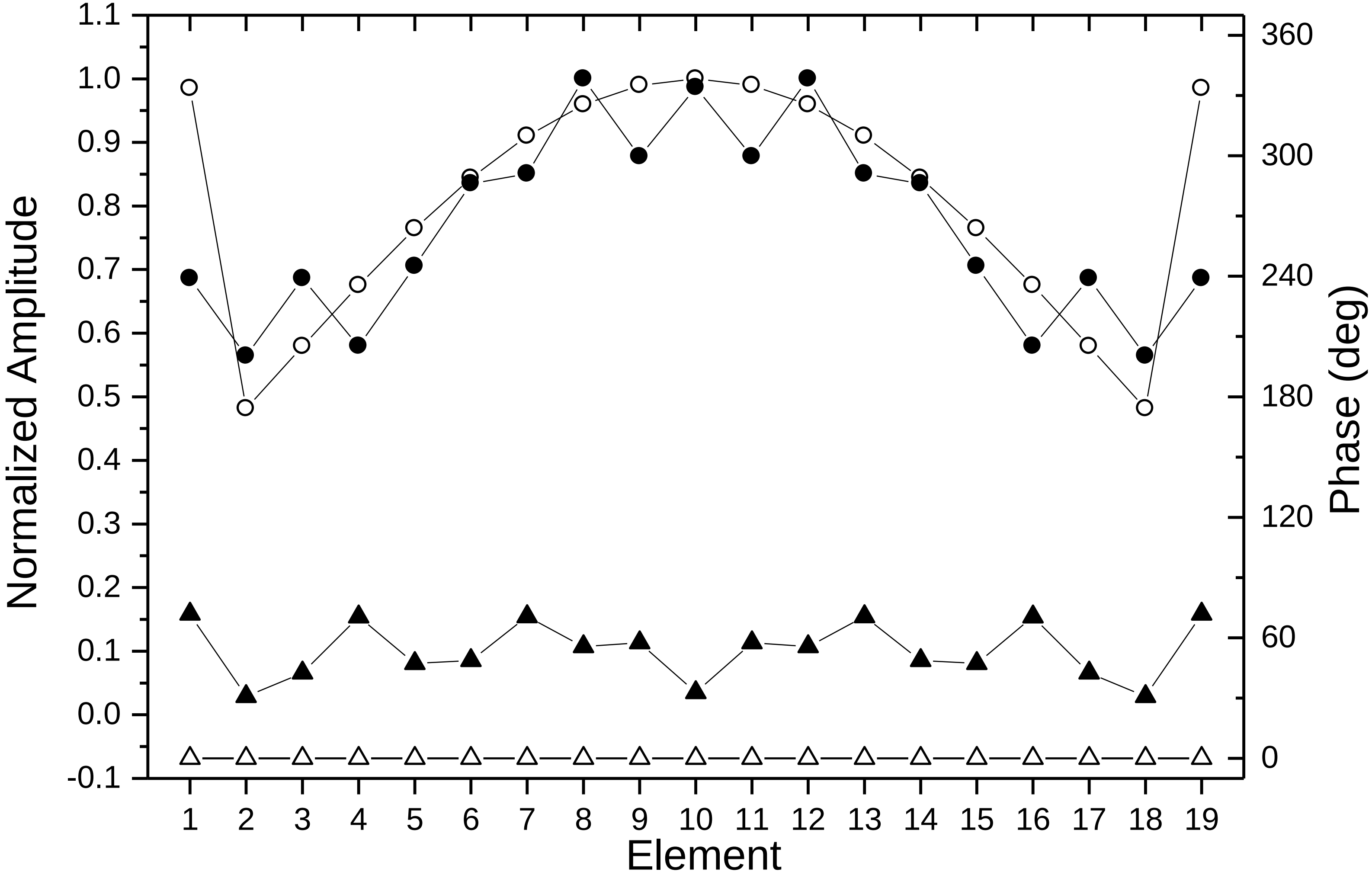
Normalized Amplitude
Phase (deg)
Element
1.1
1.0
0.9
0.8
0.7
0.6
0.5
0.4
0.3
0.2
0.1
0.0
-0.1
360
300
240
180
120
60
0
1 2 3 4 5 6 7 8 9 10 11 12 13 14 15 16 17 18 19

Fig. 1

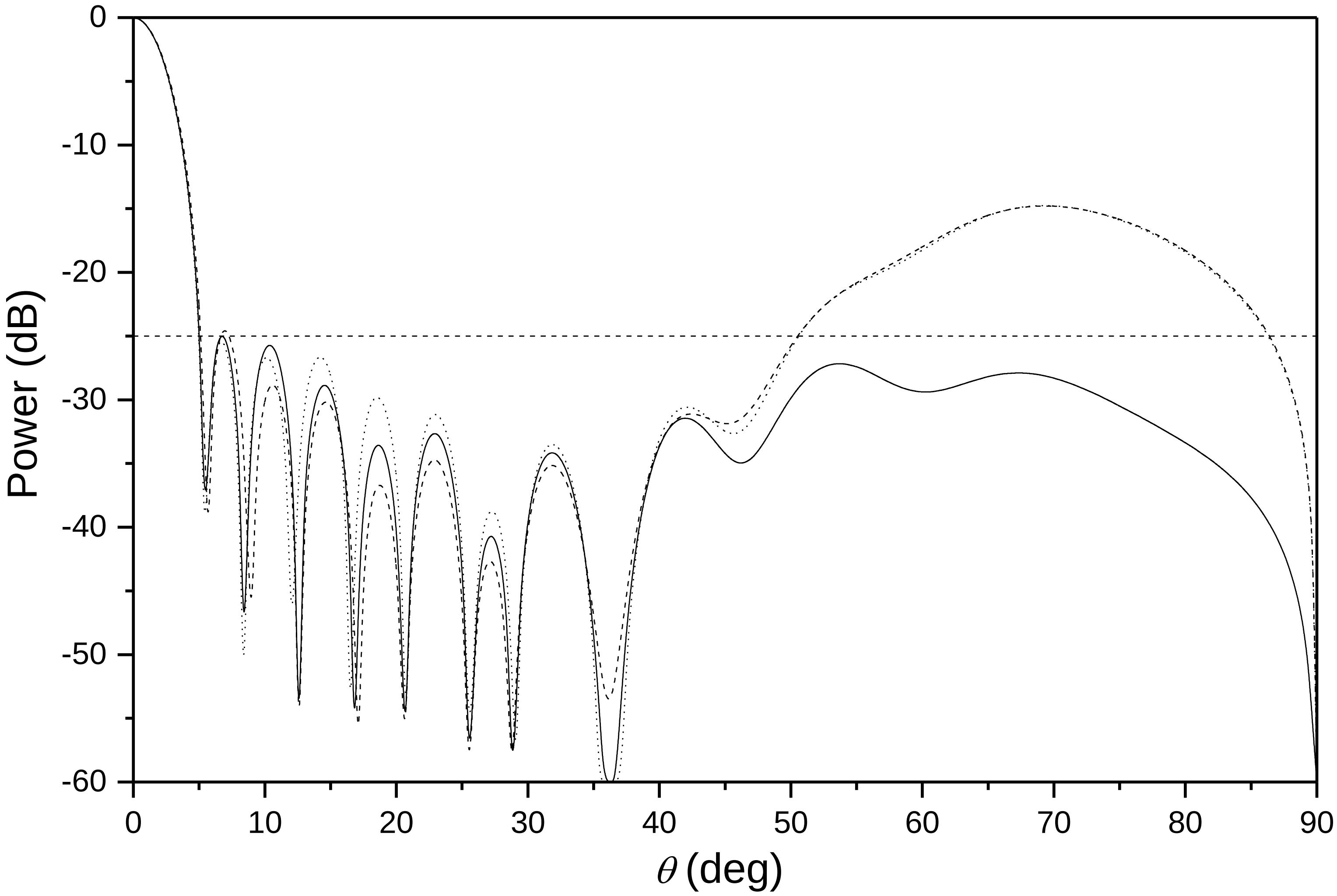

Fig. 2

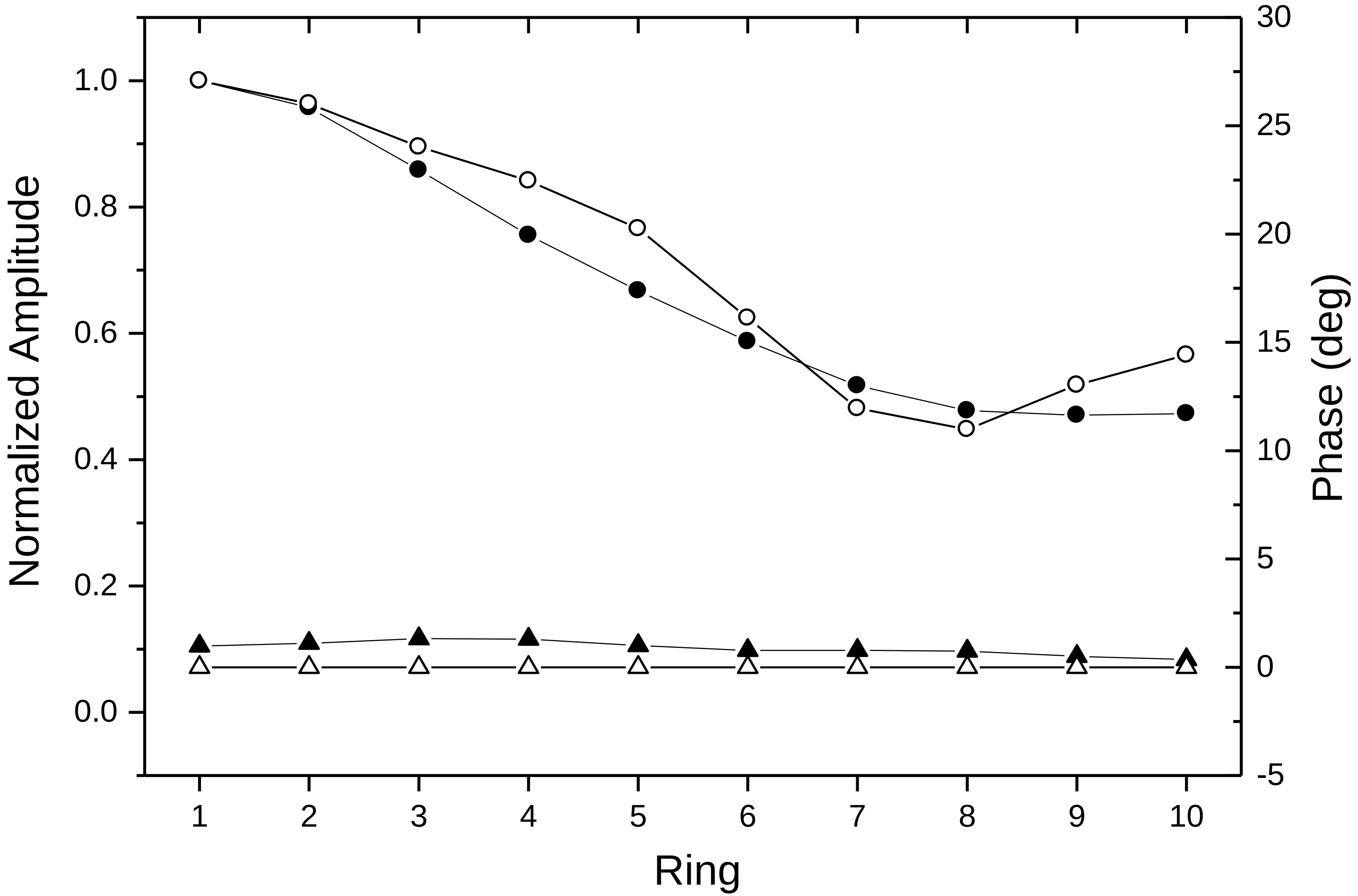

Normalized Amplitude
1.0
0.8
0.6
0.4
0.2
0.0
Phase (deg)
30
25
20
15
10
5
0
-5
1
2
3
4
5
6
7
8
9
10
Ring

Fig. 3